Journal of Additive Manufacturing Technologies
DOI: 10.18416/JAMTECH.2111581

Infinite Science | Publishing

Directed energy deposition process development for functionally gradient Copper-Inconel 718 materials

M. E. Balkan [1*], E. Aydoğan [2], M. Işık [3], B. Derin [4], B. Koç [1]

[1] *Faculty of Engineering and Natural Sciences, Manufacturing Engineering, Sabanci University, 34956 Tuzla, Istanbul, Turkey*
[2] *Faculty of Engineering, Metallurgical And Materials Engineering, Middle East Technical University, 06800 Cankaya, Ankara, Turkey*
[3] *Sabanci University Integrated Manufacturing Technologies Research and Application Center, Teknopark Istanbul, 34906 Tuzla, Istanbul Turkey*
[4] *Metallurgical and Materials Engineering Department, İstanbul Technical University, 34469 Maslak, Istanbul, Turkey*
[*] *Corresponding author, email: mbalkan@sabanciuniv.edu*

Abstract

Bimetallic systems are widely used in applications requiring combination of different material properties, such as in the aerospace industry, nuclear industry. Especially in rocket propulsions, Copper-Inconel alloys provide significant advantages due to the excellent heat conduction and wear resistance of Copper alloy and corrosion and oxidation resistance of the Inconel alloy. However, bimetallic systems produced by traditional methods could fail because of different material behavior under extreme conditions. Recently, additive manufacturing (AM) is considered as a promising technique to produce functionally graded materials (FGM) for large and complex parts with a short lead-time. In this paper, we aim to develop a CuSn10-Inconel 718 functionally gradient material using directed energy deposition (DED) AM process to elucidate the relation between process parameters and the microstructure. The DED process parameters have been optimized to produce desired FGM structure, and thermodynamic calculations have been conducted to investigate undesired phases within the gradient structure. Microstructure and the elemental composition of the gradient material have been investigated using scanning electron microscopy (SEM) and energy dispersive spectroscopy (EDS). The study aims to combine the experimental and thermodynamic computational modeling, to demonstrate the viability of assessment through computational work for a gradient material additively manufactured by DED processes.

Keywords: Additive manufacturing, Thermodynamic computational modeling, Directed energy deposition, Microstructure

1. Introduction

Metal alloys or composite materials have improved the properties of constituent materials, their properties are mostly homogenous throughout the structures. However, in certain critical applications, different functionalities and material properties are needed at different locations of the part [1]. Metal-Ceramic composites for thermal barrier structures, heat protection sheets, low temperature resistant nickel-titanium thermal barriers are some examples of multi material structures used in aerospace, jet engine control systems and space shuttle projects [2]. Usually, parts possessing long thermal fatigue and resistant to thermal cracks and erosion are needed for nuclear applications. To overcome these challenging requirements, multi material structures could be used. In general, the parts utilized in aerospace and nuclear industries experiences severe thermal gradients, and such phenomena demands different structural behavior in different locations of the structure. For a single part, a simultaneous demand for oxidation, corrosion, and wear resistances, and high thermal conductivity shall sometimes be needed in different regions of the structure [3-6] and thus bringing the need of combining different materials in a single structure [3-7].

To combine different materials, traditional fusion welding methods are still of use. This process needs a transaction layer between two different materials to avoid the occurrence of cracking [8]. Friction stir welding (FSW) is a fusion welding method, and is used to manufacture multi material structures. Nonetheless, using FSW and traditional fusion welding processes, the formation of the cracks, large heat affected zone and other microstructural defects are inherently triggered due to massive heat input. FSW process also leads into thermal residual stresses in the final structure due to local small transition zone between two unsimilar materials, but, one can overcome this problem by introducing a larger gradient zone between two materials [9-15]. Since the directly bonded multi material structures suffers from cracking and delamination issues originated from dissimilar material properties of the combining metals, functionally graded materials (FGM) were proposed. By using such materials, creating gradual changes in material properties is realized, and above stated problems be eliminated [16], though, research on the FGM method is still ongoing.

The need of advanced structures for the gas turbine engine and rocket engine parts is steadily becoming worldwide as mission profiles for such technologies gets harder. To this end, high thermal conductivity for faster cooling, wear and corrosion resistance, high yield strength properties are needs to be merged in a single structure. Nickel based alloys, especially Inconel 718, holds excellent mechanical properties such as high tensile, creep, fatigue and rupture strength on high temperatures and are widely used in aerospace industry [17]. Recently, the copper alloys have been started to be used in rocket propulsion to increase material efficiency with their excellent thermal conductivity. In regeneratively cooled rocket engines, GRCop-84 is utilized as the nozzle liner material [18,19]. Similarly, CuSn10 also stands for being a promising material in applications of cooling channels, fusion reactors, aviation industries due to its high heat conduction feature and wear resistance [20].

Additive manufacturing (AM) enables to manufacturing of multi-material structures in a post processing free state [21-23]. Especially, one of the additive manufacturing methods, directed energy deposition (DED) not only can fuse two different metals but also can produce functionally graded materials. In DED, the metal powder and laser are simultaneously released out of the same nozzle, thus, powder is being fed continuously along the melt pool [24]. This method is easily adapted to manufacture FGM, since two or more powder hoppers are already present in DED. By doing so, compositional graded structure manufacturing becomes available since one can change the powder composition between layers [25,26]. Another advantage of the DED, the process provides a unique heterogeneous structure where the mechanical and thermal properties of the part vary throughout the structure itself to withstand severe environmental conditions in multiple directions [27]. However, undesired intermetallic phases in the microstructure still are a side product of the DED process since it is essentially a fusion process. This issue is widely witnessed phenomenon in different metal combining processes and attempted to be addressed by several scholars [28-31]. Main focus for these studies has been the process optimization to increase mechanical and microstructural properties of the bimetallic structures. In the literature, there haven't been any studies investigated the relation between thermodynamic modeling of the structure and data gathered from experimental work, to examine if it is possible to determine process parameters. Also by using DED method, one can achieve different mechanical properties along the structure according to the building direction and manufacturing larger parts is possible with DED. Thus DED process is used for creating FGM CuSn10-IN718 for this study.

For FGM structures, understanding the relation between the process parameters and the microstructural behavior in the transition areas hold a great deal of importance. For the transition areas between two materials, the most problematic defections happens in fully mixed region. That's why in this study, 50%-50% CuSn10-Inconel718 composite is produced by using DED method. Process parameters for FGM structure is developed whereas the microstructure, phase composition, elemental composition have been investigated using scanning electron microscopy (SEM) and energy dispersive spectroscopy (EDS). There has already been some literature on the trial and error on process parameters. However, to the best of our knowledge, there is a shortage of the study in the literature combining both experimental and modeling work. In this study, an innovative approach has been used where the confirmation of thermodynamic calculations, CALculation of PHAse Diagrams (CALPHAD) modeling has been done via experimental work. Phases in the gradient zone, has been compared with the data gathered from the CALPHAD to show the eligibility of predicting the data that obtained from the experimentally investigated structures with thermodynamic calculations.

2. Material and methods

By combining low-cost high thermal conductivity copper alloy with high strength corrosion resistant nickel alloy, the desired thermomechanical properties can be achieved. This motived us to use two aerospace materials Inconel 718 and CuSn10 for this study.

The gradient material is fabricated via DED processing with double hoppers (DMG Mori Seiki LASERTEC 65 DED Hybrid) and using In 718 powder (Oerlikon, Freienbach, Switzerland) with a particle size ranging between 106 - 45 µm and CuSn10 powder (Schlenk, Roth, Germany) with a mesh size of 63 - 160 µm on C45 type Carbon steel substrate. The chemical compositions of the metal powders are given in Table 1.

Table 1. Metal powder chemical compositions in weight percent.

	Inconel 718	CuSn10
Ni	53.9	-
Cr	18	-
Fe	18	-
Nb	5	-
Mo	3	-
Al	0.6	-
Ti	1	-
Cu	-	90
Sn		10
P		0.07

A high-powered fiber-coupled diode laser creates a melt pool on which metal powder is deposited directly into. Whole manufacturing process was executed under argon shielding and carrier gas. The two different hoppers simultaneously deliver the multiple metal powders, and thereby enable the fabrication of multi-material structure.

2.1. Process parameters development

To produce high quality structures, optimizing the main process parameters such as laser power, scan speed, hatch distance, powder flow rate and layer thickness is required. Moreover, the dissimilarity between the thermal properties of multi-material structures is an aspect that needs to be taken into account. These intrinsic properties are the heat capacity, melting point, and coefficient of linear thermal expansion in different materials. The material process parameters development is started by 50%-50% Inconel 718-CuSn10 single track trials. To determine the starting parameters set, a variant of the total energy input per volume (E) equation is used. Total energy input equation (1) contains the laser power (P), scan speed (v), layer thickness (h) and hatch distance (t), since these are the parameters that have the greatest impact on the energy density. Total energy input unit is J/mm^3 [32,33].

$$E = \frac{P}{v * h * t} \tag{1}$$

For single track trials, hatch distance parameter becomes irrelevant and by removing the hatch distance from the equation, energy input per area is used to obtain initial process parameters. Prior to this work, we have optimized the process parameters for In 718 and CuSn10 separately with experimental studies. For initial energy per area value selection, these optimized single material process parameters such as laser power, layer thickness and scan speed are taken into account and calculated 107.14 j/mm^2 and 164.94 j/mm^2 respectively, for Inconel 718 and CuSn10 alloys. Thus 136.09 j/mm^2 is calculated to achieve a gradient structure and related process parameter values are selected to give the same total energy input per area. Then, by using different total energy input per area values, nine single track structures has been manufactured to achieve the optimized single track. Fig. 1a represents the selected single track out of nine single track trials which are fabricated using different laser power and powder feed parameters. The best single track is selected by examining the specimens from the aspects of the bonding quality, and formation of delamination, dilution and steep edges, and is seen on Fig. 1a, process parameters has been given in Table 2. Laser power and powder feed parameters from the selected single track structure are taken into account for 50%-50% Inconel 718-CuSn10 cubic structure, since material development process indicates to stabilize good bonding with the substrate first. However, the final laser power parameter for the cubic structure is changed due to achieve a gradient structure with better mechanical integrity. Calculated total energy input per volume for the single material optimization of Inconel 718 and CuSn10 are used as 71.42 j/mm^3 and 122.18 j/mm^3, respectively, for such optimization. These values have been calculated after optimizing the process parameters for In 718 and CuSn10 separately. For such calculation, Equation 1 is used.

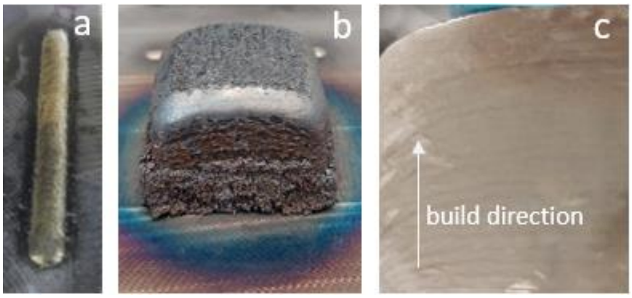

Fig 1. Inconel 718 – CuSn10 gradient structures: (a) optimized single track, (b) optimized 30x30x30 mm cubic, (c) cross section view of cubic in build direction.

Fig. 1b shows 3D view and Fig 1c shows cross section view of 30mm x 30mm x 30mm Inconel 718-CuSn10 50%-50% graded structure that has been manufactured by the DED process. The optimized processing parameters are given in Table 3.

2.2. Characterization of Inconel 718-CuSn10 gradient structure

The sample is removed from the substrate using automatic double column bandsaw machine (Kesmak KYS 400 x 600). The manufactured FGM sample was sectioned across the building axis to observe the cross-section of the specimen. The cross section was wet-polished using SiC grinding papers up to 4000 grit, then followed by cloth polishing using 1 μm aluminum-oxide suspension media. A solution containing 40% HCI (hydrochloric acid), 30% CH3COOH (acetic acid), and 30% HNO3 (nitric acid) was prepared for chemical etching of mirror-polished sample. Etching was then performed by the prepared chemical solution for 15 seconds to expose the microstructural features.

Table 2. Optimized process parameters of gradient single track.

	Laser Power (J/s)	Layer Thickness (mm)	Scan Speed (mm/s)	Powder Feed (g/min)	Total Energy Input Per Area (j/mm^2)
No:5	2274	1,045	14,58	15,77	149.21

Subsequent to the polishing procedure, the gradient structure is examined with scanning electron microscope (SEM) by using field emission gun (FE-SEM, Zeiss Leo Supra VP 35) at 20kV accelerating voltage. Energy dispersive X-ray spectroscopy (EDX) (Oxford Instruments, Oxford, UK) was performed to generate elemental composition and evaluate the compositional variation as well as diffusion throughout the selected zones.

Table 3. Optimized process parameters of gradient cubic structure.

	Laser power (J/s)	Scan Speed (mm/ s)	Hatch distance (mm)	Layer thickness (mm)	Total energy input per volume (j/mm^3)
Optimized Process Parameters	2179	14,58	1.46	1.045	97.93

2.3. Thermodynamic computation

A CALPHAD model was performed by using "Equilib" module of FactSage™ 8.1 thermochemistry software [34] to predict the possible phases during equilibrium cooling of 50:50 mixture (by weight) of CuSn10:Inconel718 alloy from molten state. The thermodynamic data for the calculation was taken from FSstel solution database.

3. Results and discussion

Microstructural investigations shows that the gradient structure without detection of any defects have been successfully fabricated. Both Inconel 718 and CuSn10 having the same unit cells as face centered cubic, improved the compatibility and natural transition achieved between two alloys. SEM images has been given in Fig. 2, captured from three different regions with 5 mm interval along build direction. In (Fig. 2 a-c) gradient zones, equiaxed structures detected with a continuous distribution, which might helped to form the good metallurgical bond throughout the structure [35]. The equiaxed structure in Fig. 2 (b) displays a coarser grain size when comparing to the Fig. 2 (a) and (c). This is related to solidification rate differences between the locations through the sample.

Throughout the manufacturing process, the FGM sample is rotated 90° between layers, i.e., a 90° hatch angle was used. It is stated that direction of the laser indicates the columnar dendrite growth direction [36]. This proves that the observed dendrite structures on the examined gradient zones are disordered while incessant between layers. In general the microstructure displays adjoined properties across the build direction of the gradient zone. In this study we have observed a dendritic structure in CuSn10 and In718 FGM material similar to studies of C. Shang, et al. and S. Scudino et al. [35,37]. Several zones selected through build up direction randomly and EDS area mapping conducted. It is concluded that the elemental composition across the gradient zone follows the designed composition without major divergence. Fig. 3 shows the related elemental composition through a randomly selected zone. The designed composition and the actual composition measured by EDS (weight percent average of EDS area mapping zones) are tabulated in Fig. 3b, presenting that the planned composition for the gradient structure is nearly the same as the experimentally obtained one. The error percentage between designed and achieved composition can be justified by the limitations of the EDS process [38]. (Fig. 3 c-h) demonstrates homogenous gradient structure with evenly distributed Ni, Cu, Cr, Fe, Sn, Nb elements.

Fig. 4 represents the phase changes of the alloy under equilibrium condition and within a temperature range from 1700 °C to 200 °C. The single liquid melt is first separated into two immiscible liquid phases with different compositions at ~1550 °C. According to the calculation, the formation of the Ni-rich first phase particles at ~1200 °C (fcc Ni-Fe-Cr-Cu-Nb-Sn-Ti-Al system) is followed by the formation of Cu-rich second phase particles (fcc Cu-Ni-Mo-Sn-Fe-Cr-Al system) at ~1050 °C. The solidification of both nickel-rich and copper-rich alloys is complete at ~1050 °C and ~850 °C, respectively. A Cr-rich bcc phase formation is observed just before the end of the last liquid phase at ~896 °C. After the liquid phase is depleted, the other possible phases expected to form during cooling are the high-temperature form of Ni3Sn2, Ni3Ti, the low-temperature form of Ni3Sn, Ni-rich fcc phase, P-phase and Laves phase, respectively.

It is noteworthy that carbon and phosphorus, which are present in very small amounts in Inconel718 and CuSn10 alloys, respectively, were not included in the present calculation. The effect of both elements, as well as non-equilibrium behavior of the alloy during cooling will be discussed after a comprehensive microstructure characterization of the samples.

4. Conclusions

Functionally graded Inconel 718 – CuSn10 structure have been successfully fabricated by using directed energy deposition. Single track trials gave an insight for initial process parameters since we can understand the bonding behavior of the related material by fabricating such structures. Microstructural examinations of graded structure, show no indication of distinct structural, compositional or microstructural boundaries.

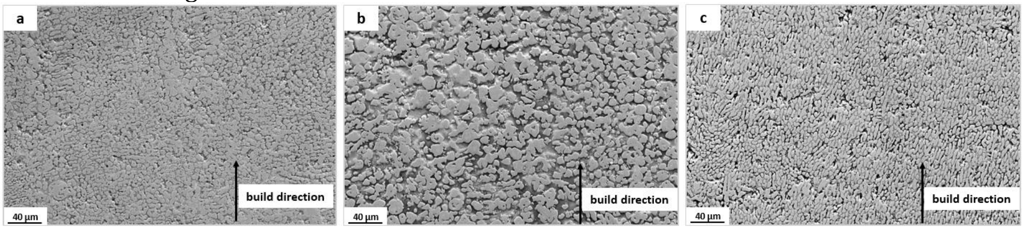

Fig 2. SEM images of gradient structure from three different regions with 5 mm interval along build direction.

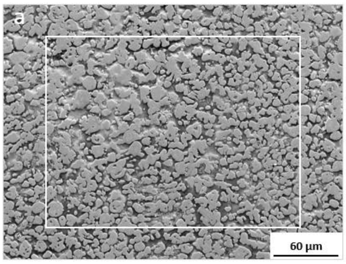

b	Designed	Achieved
Ni	26.95	21,41
Cu	45	43.21
Cr	9	8,53
Fe	9	8.26
Sn	5	2,52
Nb	2.5	1,61

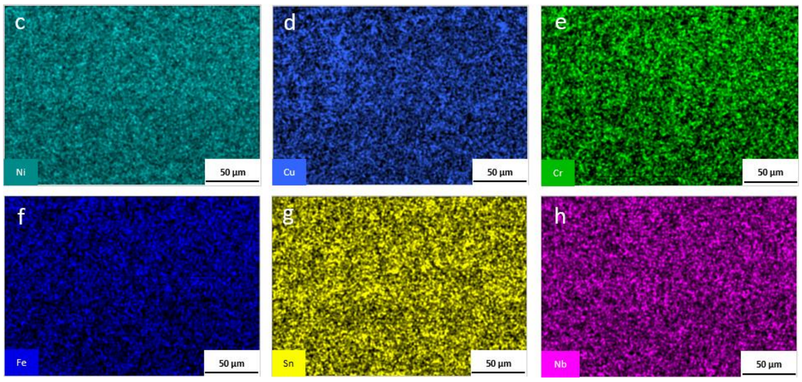

Fig 3. EDS mapping results: (a) SEM image of investigated area, (b) achieved and desired elemental compositions in weight percent, (c) EDS mapping for Ni, Cu, Cr, Fe, Sn, Nb.

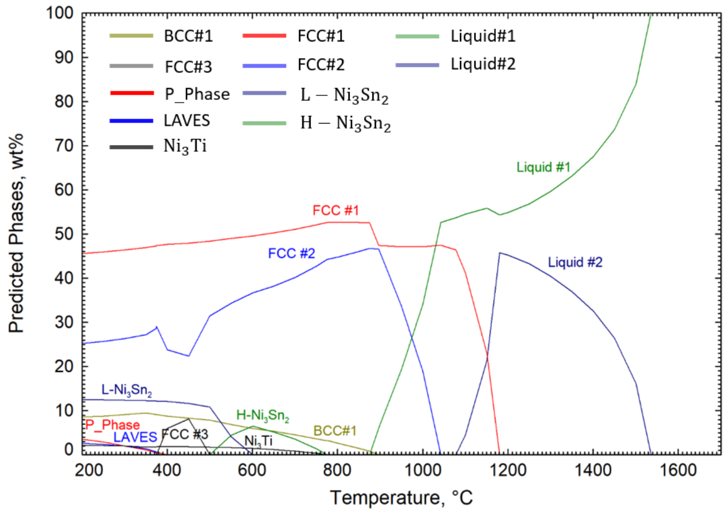

Fig 4. Equilibrum cooling calculation of 50:50 mixture (by weight) of CuSn10:Inconel718 alloy using FactSage™.

Fine dendritic structure aligned along building direction was observed without any delamination. By using CALPHAD method, thermodynamic calculations have been conducted to predict and evaluate the stable phases within 50%-50% Inconel 718-CuSn10 gradient structure while EDS mapping shows evenly distributed elemental composition throughout the structure. This study shows the feasibility of fabricating gradient nickel-copper alloy using directed energy deposition. Furthermore it has been demonstrated that CALPHAD based thermodynamic computation is viable for gradient structure design purposes. It is foreseeable that by using such innovative design methodologies, next generation aerospace & nuclear materials will have higher mechanical integrity.

Acknowledgments

Technical support from Fatih Polat and Ferdows Afghah is acknowledged.

Author's statement:

Conflict of interest: Authors state no conflict of interest. Informed consent: Informed consent has been obtained from all individuals included in this study. Ethical approval: The research related to human use complies with all the relevant national regulations, institutional policies and was performed in accordance with the tenets of the Helsinki Declaration, and has been approved by the authors' institutional review board or equivalent committee.

References

1. A. Mortensen, S. Suresh, Functionally graded metals and metal-ceramic composites: part 1 Processing, Int. Mat. Rev. 40 (6) (1995) 239e265.
2. Gururaja Udupal, S.Shrikantha rao, K.V.Gangadharan, International Conference On Advances In Engineering, Science And Management 2012
3. S. Suresh, A. Mortensen, Fundamentals of Functionally Graded Materials, IOM Communications Ltd, London, 1998.
4. M. Shakil, M. Ahmad, N.H. Tariq, B.A. Hasan, J.I. Akhter, E. Ahmed, M. Mehmood, M.A. Choudhry, M. Iqbal, Microstructure and hardness studies of electron beam welded inconel 625 and stainless steel 304L, Vacuum 110 (2014) 121e126.
5. V. Birman, L.W. Byrd, Modeling and analysis of functionally graded materials and structures, Appl. Mech. Rev. 60 (5) (2007) 195.
6. Z. Sun, J.C. Ion, Review laser welding of dissimilar metal combinations, J. Mat. Sci. 30 (1995) 4025e4214
7. F. Findik, Recent developments in explosive welding, Mat. Des. 32 (3) (2011) 1081e1093.
8. R.W. Messler, Principles of Welding: Processes, Physics, Chemistry, and Metallurgy, John Wiley & Sons, Inc., New York, 1999.
9. A. Bandyopadhyay, B. Heer, Additive manufacturing of multi-material structures, Mater. Sci. Eng. R Rep. 129 (2018) 1–16.
10. M. Fazel-Najafabadi, S.F. Kashani-Bozorg, A. Zarei-Hanzaki, Joining of CP-Ti to 304 stainless steel using friction stir welding technique, Mater. Des. 31 (10) (2010) 4800–4807.
11. Z. Sun, R. Karrpi, The application of electron beam welding for the joining of dissimilar metals: an overview, J. Mater. Process. Technol. 59 (1996) 257–267.
12. H.C. Chen, A.J. Pinkerton, L. Li, Fibre laser welding of dissimilar alloys of Ti-6Al-4V and Inconel 718 for aerospace applications, Int. J. Adv. Manuf. Technol. 52 (2010) 977–987.
13. S.A. David, T. Debroy, Current issues and problems in welding science, Science 257 (5069) (1992) 497–502.
14. D.C. Hofmann, J. Kolodziejska, S. Roberts, R. Otis, R.P. Dillon, J.-O. Suh, Z.-K. Liu, J.-P. Borgonia, Compositionally graded metals: a new frontier of additive manufacturing, J. Mat. Res. 29 (17) (2014) 1899e1910.
15. J.J. Sobczak, L. Drenchev, Metallic functionally graded materials: a specific class of advanced composites, J. Mater. Sci.Technol. 29 (4) (2013) 297e316
16. R.M. Mahamood, E.T. Akinlabi, Functionally Graded Materials, Springer International Publishing, AG Switzerland, 2017.
17. Special Metals Corporation: INCONEL® Alloy 718 Product Brochure, Publication Number SMC-045, (2007) September.
18. D.L. Ellis, GRCop-84: A High-Temperature Copper Alloy for High-Heat-Flux Applications, (2005) NASA Report NASA/TM—2005-213566.
19. H.C. de Groh III, D.L. Ellis, W.S. Loewenthal, Comparison of GRCop-84 to other Cu alloys with high thermal conductivities, J. Mater. Eng. Perform. (2007) 1–24.
20. K. Chen, C. Wang, Q. Hong, S. Wen, Y. Zhou, C. Yan, Y. Shi, Selective laser melting 316L/CuSn10 multi-materials: Processing optimization, interfacial characterization and mechanical property Journal of Materials Processing Tech. 283 (2020) 116701.
21. B. Heer, A. Bandyopadhyay, Compositionally graded magnetic-nonmagnetic bimetallic structure using laser engineered net shaping, Mater. Lett. 216 (2018) 16.
22. X. Mei, X. Wang, Y. Peng, H. Gu, G. Zhong, S. Yang, Interfacial characterization and mechanical properties of 316L stainless steel/inconel 718 manufactured by selective laser melting, Mater. Sci. Eng., A 758 (2019) 185–191.
23. S.L. Sing, W.Y. Yeong, Laser powder bed fusion for metal additive manufacturing: perspectives on recent developments, Virtual Phys. Prototyping 15 (3) (2020) 359–370.
24. W.E. Frazier, Metal additive manufacturing: a review, J. Mat. Eng. Perform. 23 (6) (2014) 1917e1928.
25. R. Banerjee, P.C. Collins, D. Bhattacharyya, S. Banerjee, H.L. Fraser, Microstructural evolution in laser deposited compositionally graded alpha/beta titaniumevanadium alloys, Acta Mat. 51 (11) (2003) 3277e3292.
26. P.C. Collins, R. Banerjee, S. Banerjee, H.L. Fraser, Laser deposition of compositionally graded titaniumevanadium and titaniumemolybdenum alloys, Mat. Sci. Eng. A 352 (1e2) (Jul. 2003) 118e128.
27. H. Fayazfar, M. Salarian, A. Rogalsky, D. Sarker, P. Russo, V. Paserin, E. Toyserkani, A critical review of powder-based additive manufacturing of ferrous alloys: Process parameters, microstructure and mechanical properties, Materials & Design 144 (2018) 98–128.
28. D.C. Hofmann, K.S. Vecchio, Submerged friction stir processing (SFSP): an improved method for creating ultra-fine-grained bulk materials, Mat. Sci. Eng. A 402 (1e2) (Aug. 2005) 234e241.
29. T. Qian, D. Liu, X. Tian, C. Liu, H. Wang, Microstructure of TA2/TA15 graded structural material by laser additive manufacturing process, Trans. Nonferrous Met. Soc. China 24 (9) (2014) 2729e2736.
30. H.S. Ren, D. Liu, H.B. Tang, X.J. Tian, Y.Y. Zhu, H.M. Wang, Microstructure and mechanical properties of a graded structural material, Mat. Sci. Eng. A 611 (2014) 362e369.
31. D.C. Hofmann, S. Roberts, R. Otis, J. Kolodziejska, R.P. Dillon, J.-O. Suh, A. a Shapiro, Z.-K. Liu, J.-P. Borgonia, Developing gradient metal alloys through radial deposition additive manufacturing, Sci. Rep. 4 (2014) 5357.
32. F.A. España, V.K. Balla, S. Bose, A. Bandyopadhyay, Design and fabrication of CoCrMo alloy based novel structures for load bearing implants using laser engineered net shaping, Mater. Sci. Eng. C 30 (2010) 50–57.
33. A. Simchi, H. Pohl, Effects of laser sintering processing parameters on the microstructure and densification of iron powder, Mater. Sci. Eng. A 359 (2003) 119–128.
34. C. W. Bale, E. Bélisle, P. Chartrand, S. A. Decterov, G. Eriksson, A.E. Gheribi, K. Hack, I. H. Jung, Y. B. Kang, J. Melançon, A. D. Pelton, S. Petersen, C. Robelin. J. Sangster, P. Spencer and M-A. Van Ende, *FactSage Thermochemical Software and Databases* - 2010 - 2016, Calphad, vol. 54, pp 35-53, 2016 <www.factsage.com>
35. C. Shang, C. Wang, G. Xu, C. Li, J. You Laser additive manufacturing of TA15 - Inconel 718 bimetallic structure via Nb/Cu multi-interlayer. Vacuum 169 (2019)108888
36. G.P. Dinda, A.K. Dasgupta, J. Mazumder, Laser aided direct metal deposition of inconel 625 superalloy:

microstructural evolution and thermal stability, Mat. Sci. Eng. A 509 (1e2) (2009) 98e104.

37. S. Scudino, C. Unterdörfer, K.G. Prashanth, H.Attar, N.Ellendt, V.Uhlenwinkel, J. Eckert Additive manufacturing of Cu–10Sn bronze Materials Letters 156 (2015) 202-204
38. D.B. Williams, C.B. Carter, Transmission Electron Microscopy: A Textbook for Materials Science, second ed., Springer, New York, 2009.